

Supplementary information

Lanthanide Coordination Polymers Assembled from Triazine-based Flexible Polycarboxylate Ligands and Their Luminescent Properties

Yihui Huang,^{a,b} Qilong Zhu,^{ab} Tianlu Sheng,^a Shengmin Hu,^a Ruibiao Fu,^a Chaojun Shen,^a Chunhong Tan,^{ab} Yuehong Wen^a and Xintao Wu^{*a}

^a State Key Laboratory of Structural Chemistry, Fujian Institute of Research on the Structure of Matter, The Chinese Academy of Sciences, Fuzhou, Fujian 350002, China

^b Graduate University of the Chinese Academy of Sciences, Beijing 100039, China

The corresponding author, Fax: 86-591-83714947; Tel 86-591-83719238;
Email: wxt@fjirsm.ac.cn

The synthetic route for ligand 1,3,5-triazine-2-iminodiacetic acid-4,6-bis(L-alanine) (H_4L1) and 1,3,5-triazine-2-iminodiacetic acid-4,6-biglycine (H_4L2) according to the method described in the previous literatures.¹

1,3,5-triazine-2-iminodiacetic acid-4,6-dichloride. A solution of iminodiacetic acid (5.43 g, 40 mmol) and sodium hydroxide (4.8 g, 120 mmol) in 50 ml of water was added dropwise into cyanuric chloride (7.51 g 40 mmol) in 50 ml of water at 0-5 °C under stirring. After 3 h, the pH value was adjusted to about 2 using concentrated HCl, standing at 0-5 °C for 20 min. The white crystal powder was collected by filtration, washed with water and then dried under vacuum at 35 °C, giving the product in 65% yield. $m/z = 280.05(M-H)^-$. FT-IR (KBr cm⁻¹): 3445 (vs, br), 3117 (m), 3029 (s), 2782 (m), 1778 (m), 1752 (s), 1725 (vs), 1586 (m), 1474 (m), 1399 (s), 1235 (w), 1178 (w), 1054 (s), 853 (s), 776 (m), 755 (s).

1,3,5-triazine-2-iminodiacetic acid-4,6-bis(L-alanine) (H_4L1). A solution of L-alanine (1.82 g, 20 mmol) and sodium hydroxide (2.56 g, 84 mmol) in 20 ml of water was added dropwise into the first product (2.83 g, 10 mmol) in 10 ml of water at 35 °C under stirring. After 6 h, the mixture was allowed to reflux at 105 °C for 12 h. After cooling, the pH value was adjusted to about 2 using concentrated HCl, standing at 0-5 °C for 120 min. The white powder was collected by filtration, washed with water and then dried under vacuum at 35 °C, giving the target ligand (H_4L1) in 65% yield. $m/z = 383.31 (M-H)^-$. FT-IR (KBr cm⁻¹): 3400 (vs, br), 1728 (s), 1623 (s), 1522 (s), 1452 (m), 1401 (m), 1327 (m), 1232 (w), 1077 (w), 960 (w), 789 (w).

1,3,5-triazine-2-iminodiacetic acid-4,6-biglycine (H₄L2). A solution of glycine (1.50 g, 20 mmol) and sodium hydroxide (2.56 g, 84 mmol) in 20 ml of water was added dropwise into the first product (2.83 g, 10 mmol) in 10 ml of water at 35 °C under stirring. After 6 h, the mixture was allowed to reflux at 105 °C for 12 h. After cooling, the pH value was adjusted to about 2 using concentrated HCl, standing at 0–5 °C for 120 min. The white powder was collected by filtration, washed with water and then dried under vacuum at 35 °C, giving the target ligand (H₄L2) in 85% yield. m/z = 355.21 (M–H)[–]. FT-IR (KBr cm^{–1}): 3441 (vs, br), 1720 (s), 1670 (s), 1619 (s), 1573 (s), 1443 (s), 1404 (s), 1383 (m), 1335 (m), 1294 (m), 1266 (m), 1198 (m), 1138 (m), 1043 (w), 979 (w), 922 (w), 795 (w), 750 (W), 662(m), 617 (s), 579 (m).

Scheme S1. Synthetic Procedures for Ligands.

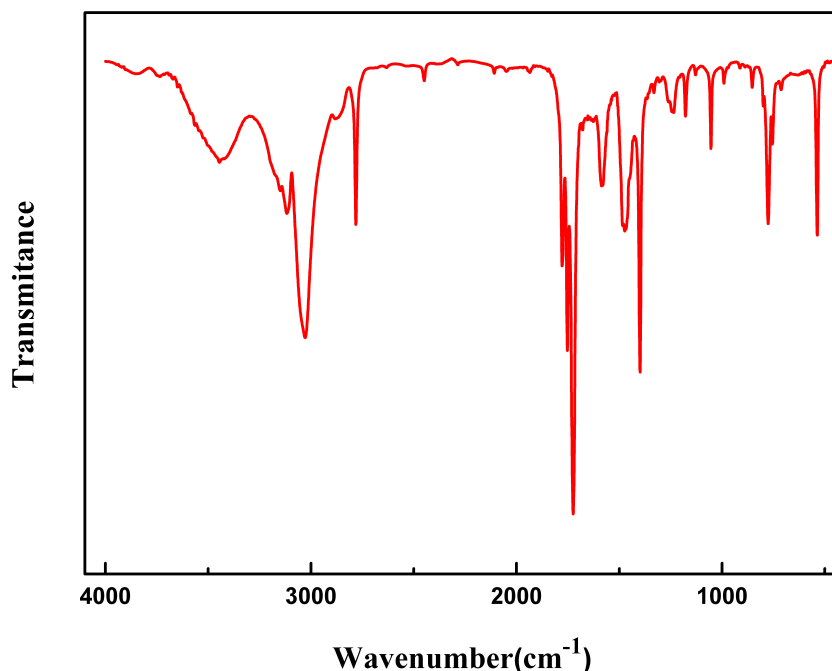
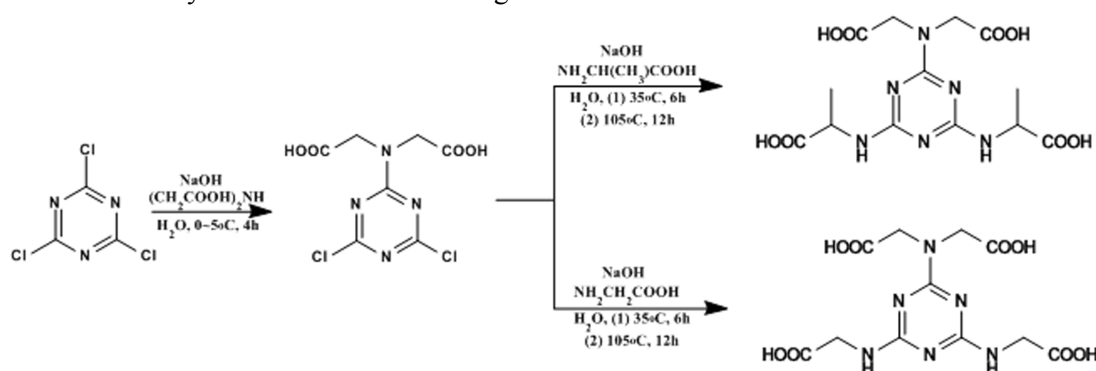


Fig. S1 FT-IR spectrum for 1,3,5-triazine-2-iminodiacetic acid-4,6-dichloride.
acid-4,6-dichloride.

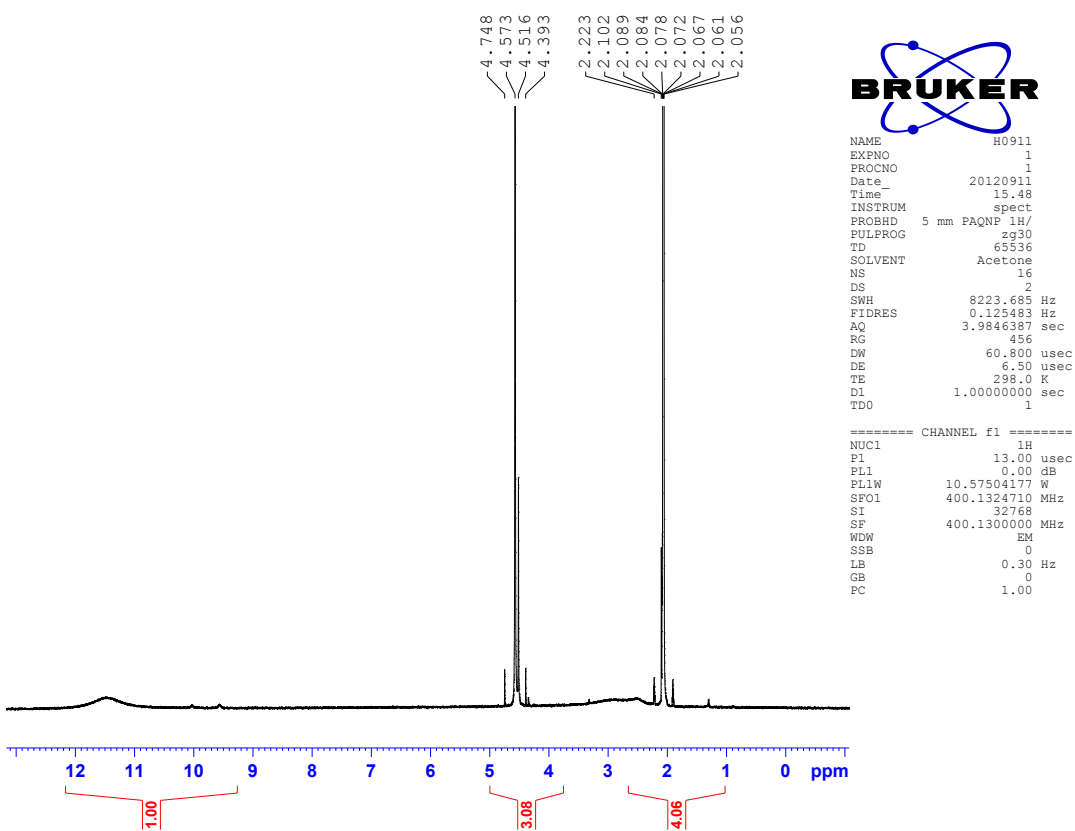


Fig. S2 ^1H NMR spectrum of 1,3,5-triazine-2-iminodiacetic acid-4,6-dichloride in acetone

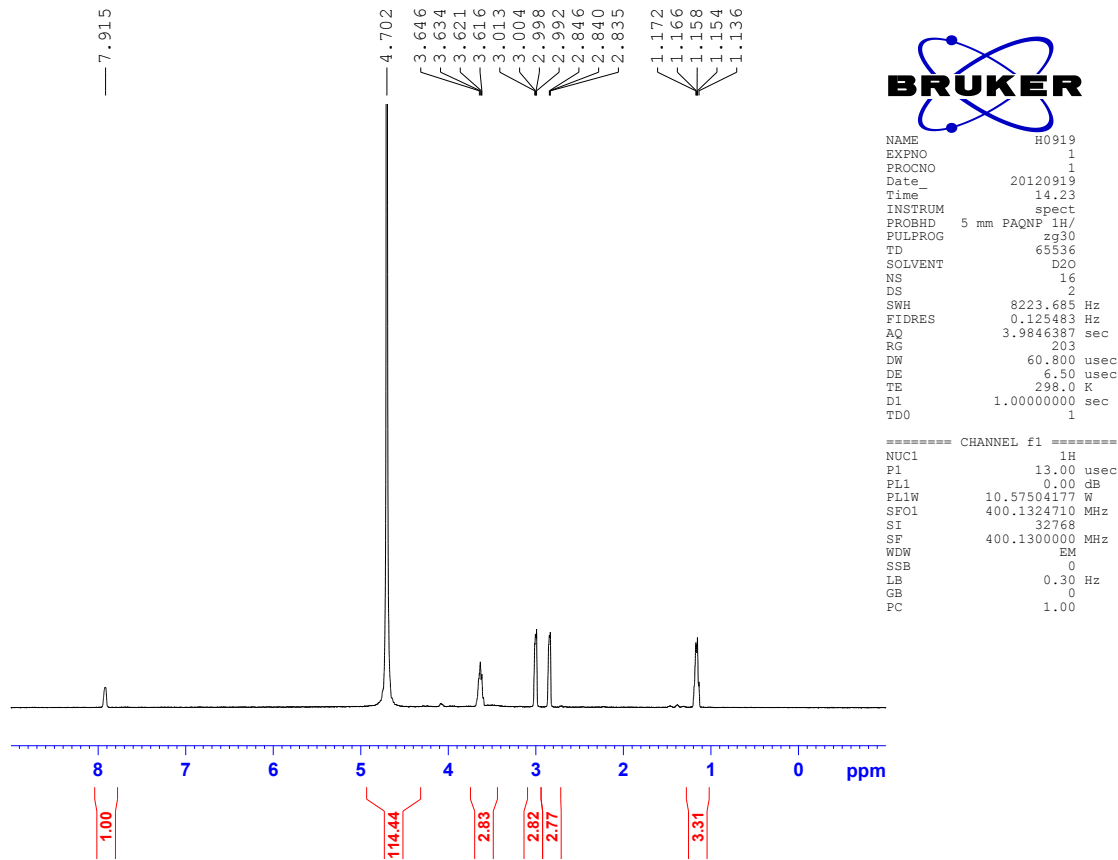


Fig. S3 ^1H NMR spectrum of 1,3,5-triazine-2-iminodiacetic acid-4,6-biglycine in D_2O

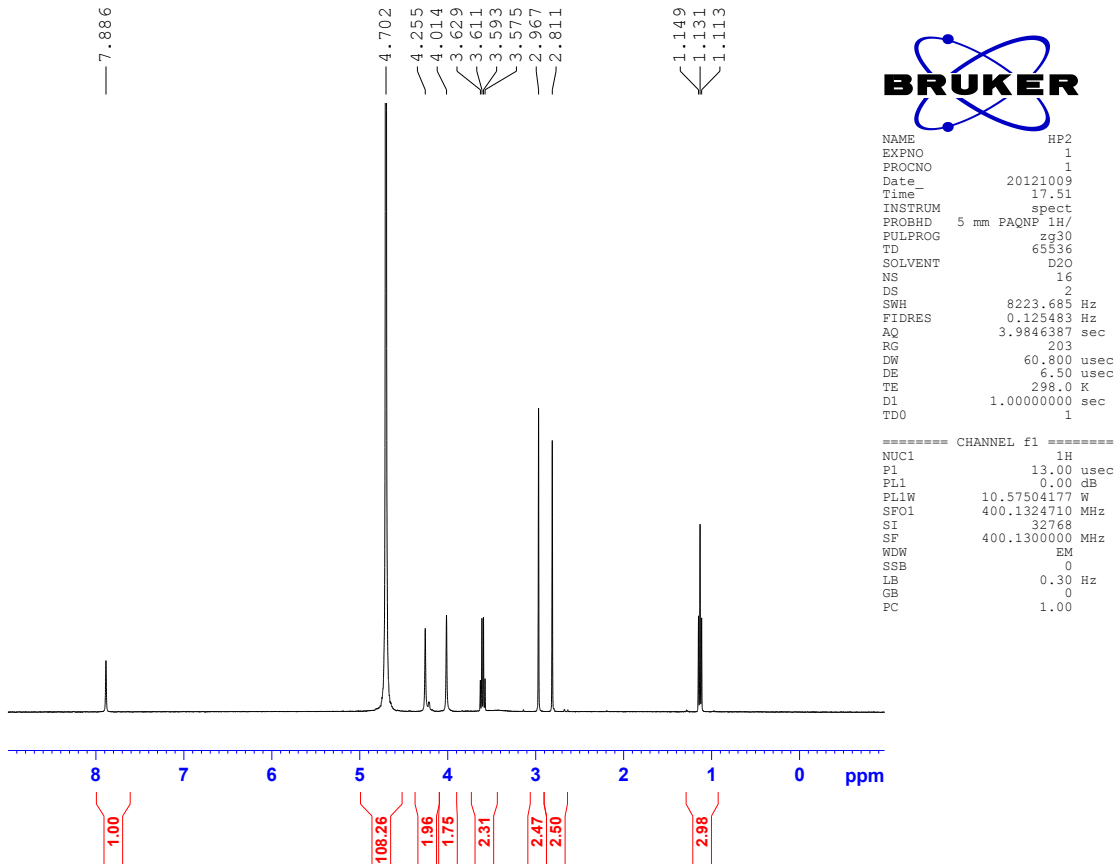


Fig. S4 ¹H NMR spectrum of 1,3,5-triazine-2-iminodiacetic acid-4,6-bis(L-alanine) in D_2O

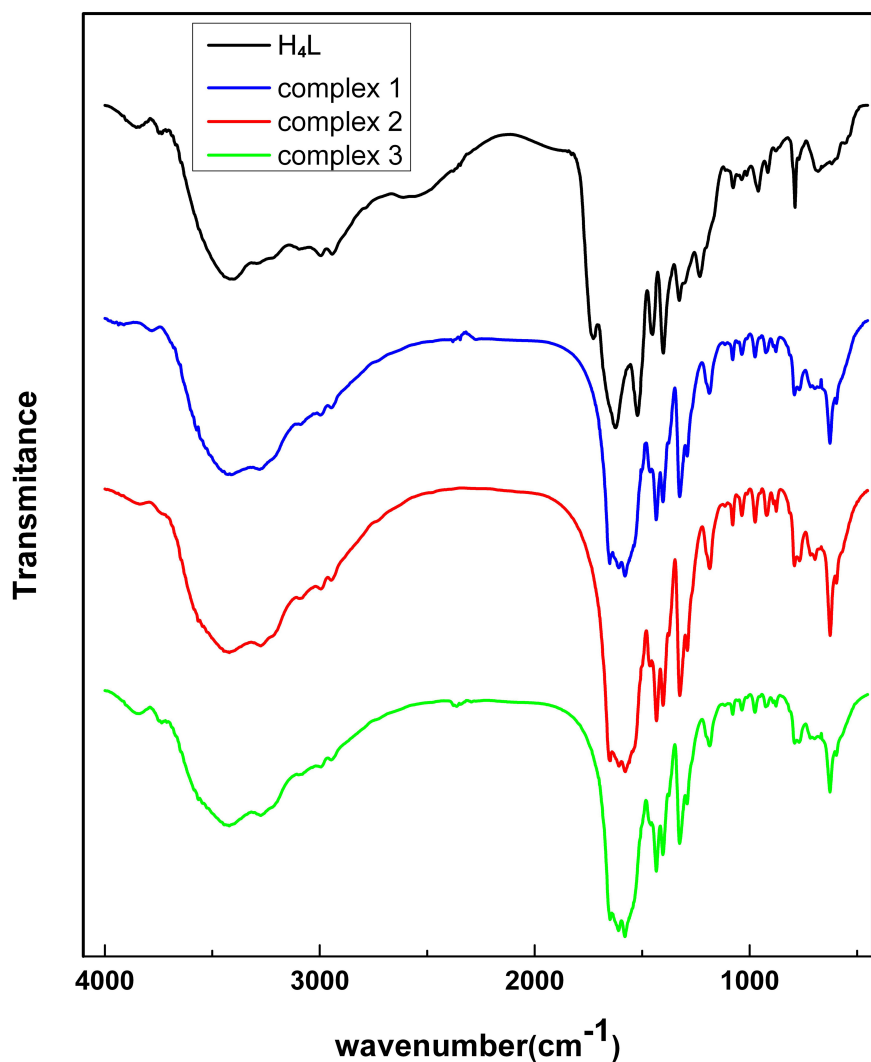


Fig. S5 FT-IR spectra for complex **1**(green), **2** (red), **3** (blue) and H_4L (black).

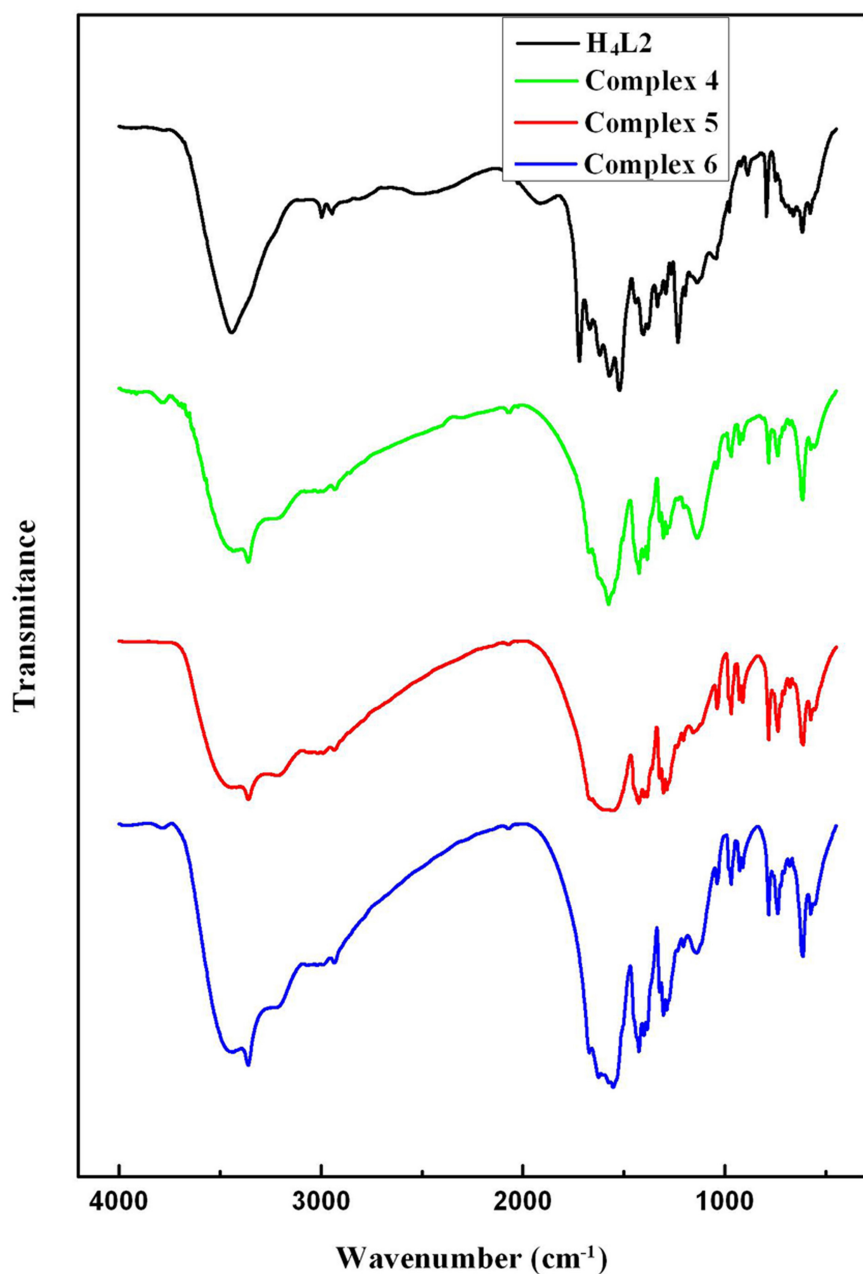


Fig. S6 FT-IR spectra for complex 4(green), 5 (red) 6 (blue) and H₄L2 (black).

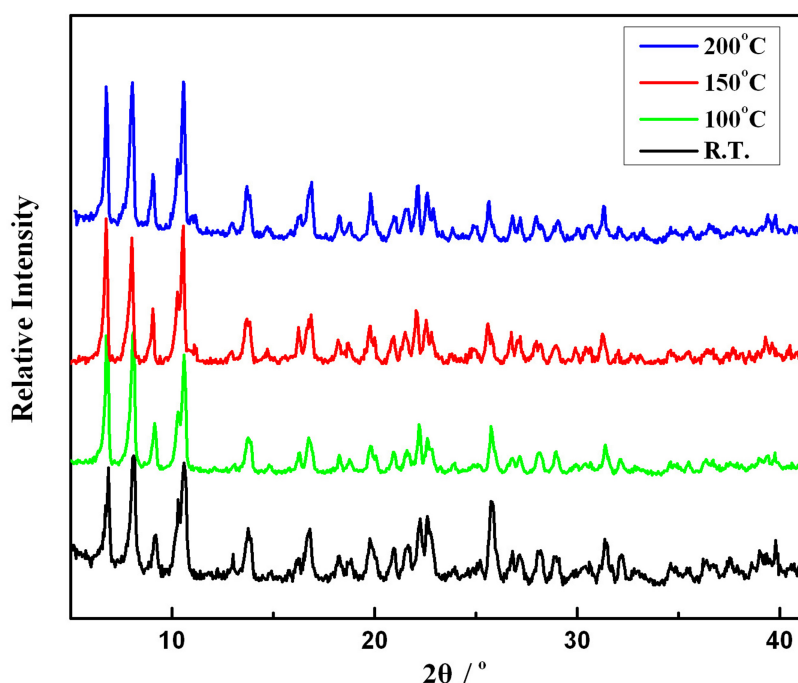


Fig. S7 X-ray powder diffraction of complex **1** (black); heated to 100 °C (red); heated to 150 °C (blue); heated to 200 °C (green).

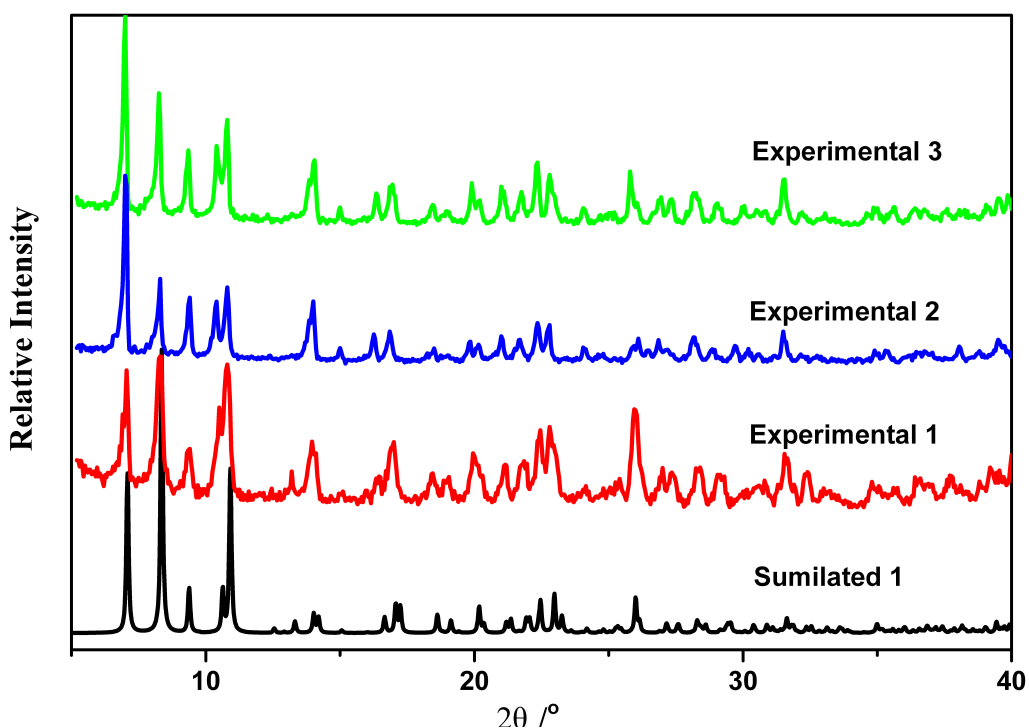


Fig. S8 Experimental PXRD patterns of complexes **1** (green), **2** (red), **3** (green) and simulated PXRD pattern from single crystal data of complex **1** (black).

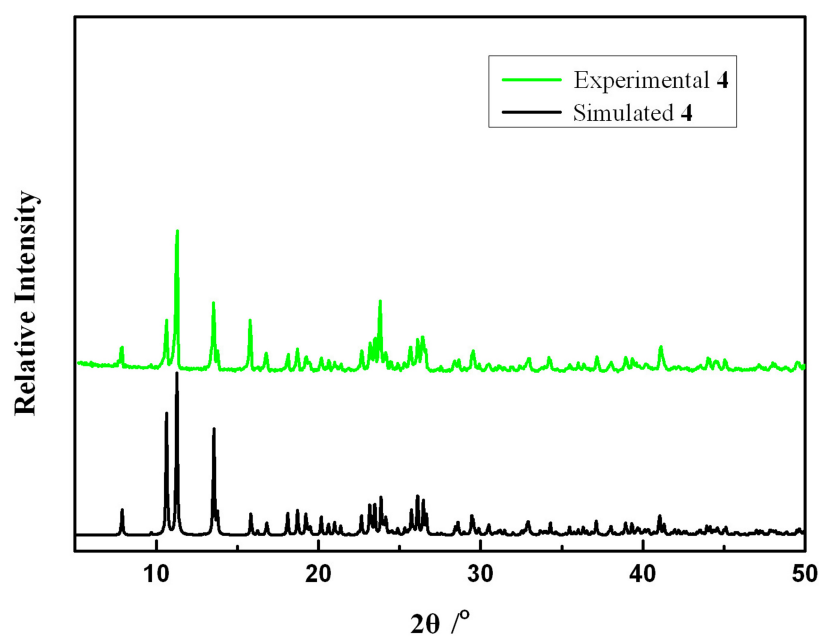


Fig. S9 Experimental PXRD patterns of complexes **4** (green) and simulated PXRD pattern from single crystal data (black).

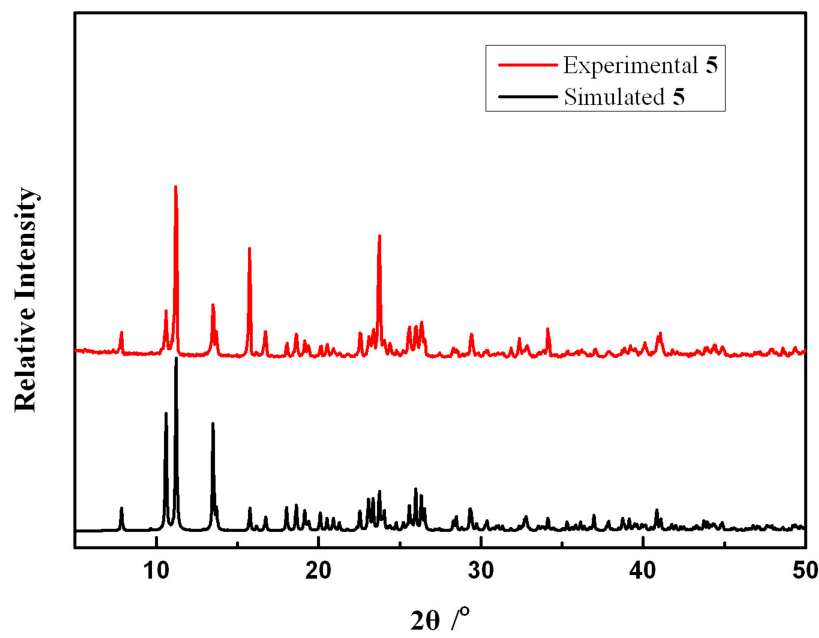


Fig. S10 Experimental PXRD patterns of complexes **5** (red) and simulated PXRD pattern from single crystal data (black).

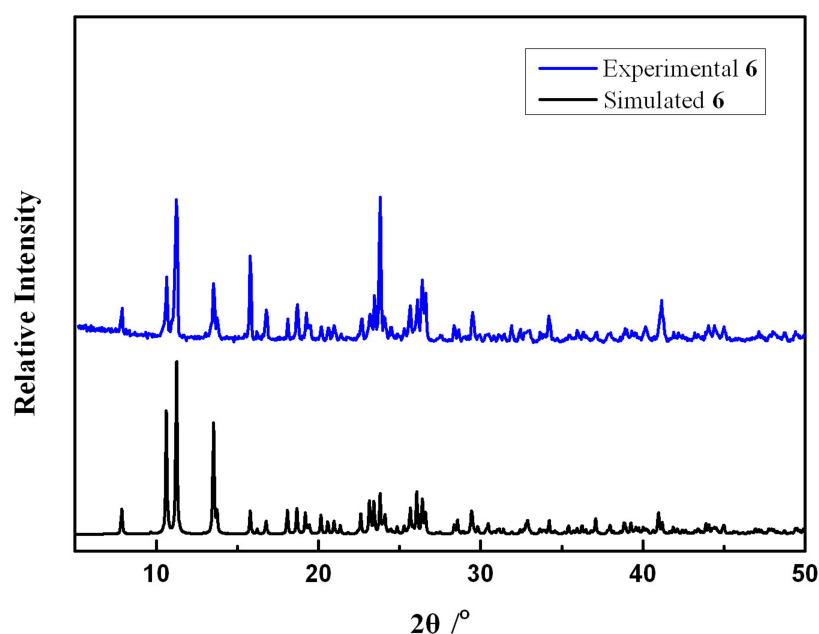


Fig. S11 Experimental PXRD patterns of complexes **6** (blue) and simulated PXRD pattern from single crystal data (black).

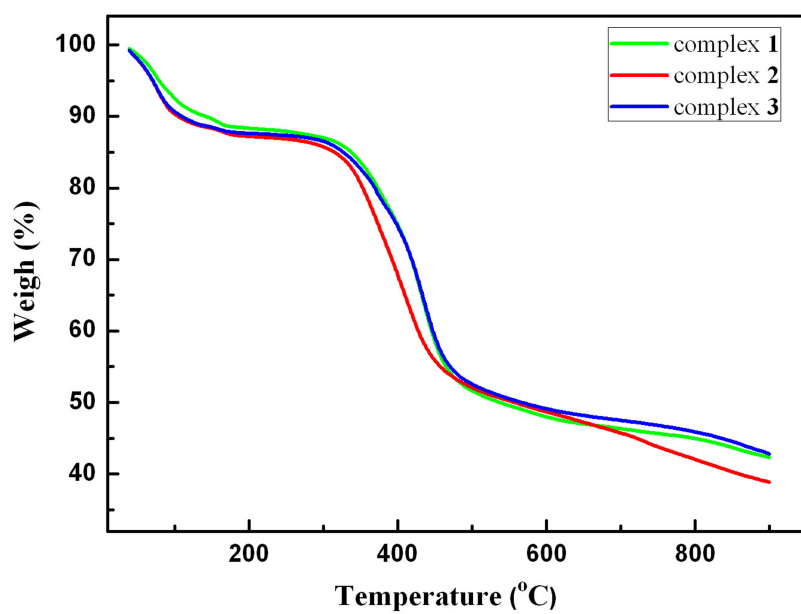


Figure S12 TGA curves for complex **1**(green), **2** (red), **3** (blue)

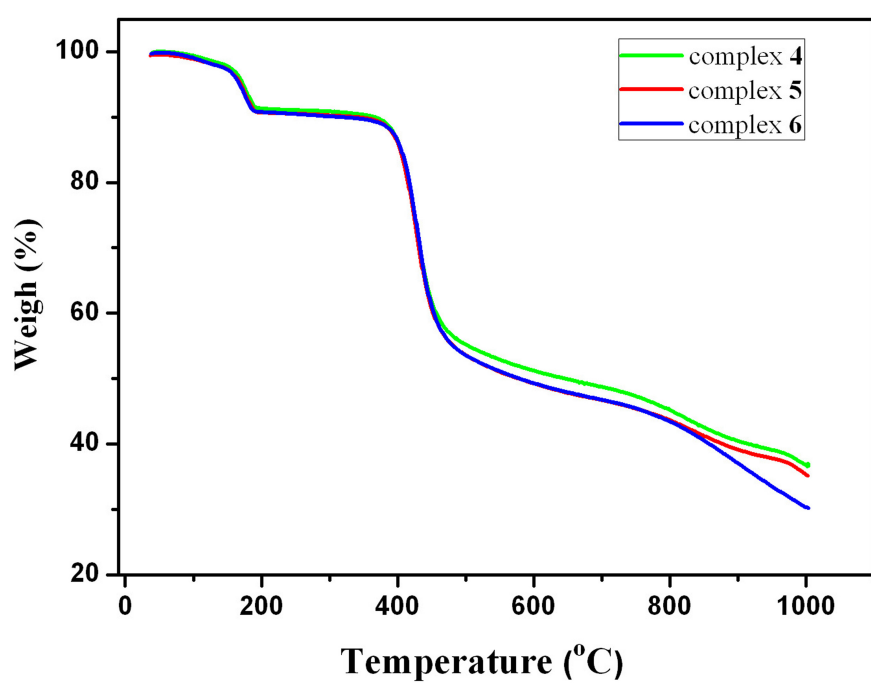


Figure S13 TGA curves for complex **4**(green), **5** (red), **6** (blue)

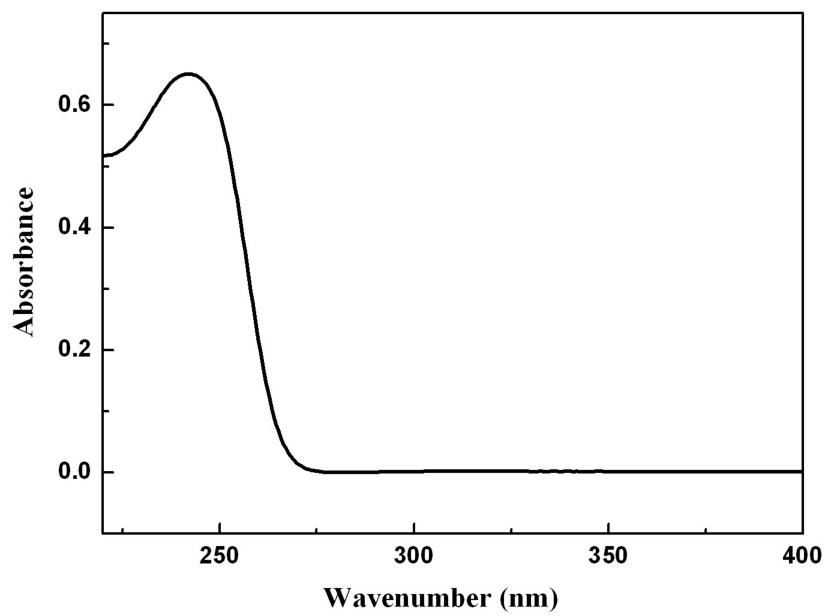


Figure S14 UV-visible spectrum for $\text{H}_4\text{L}1$ in aqueous solution.

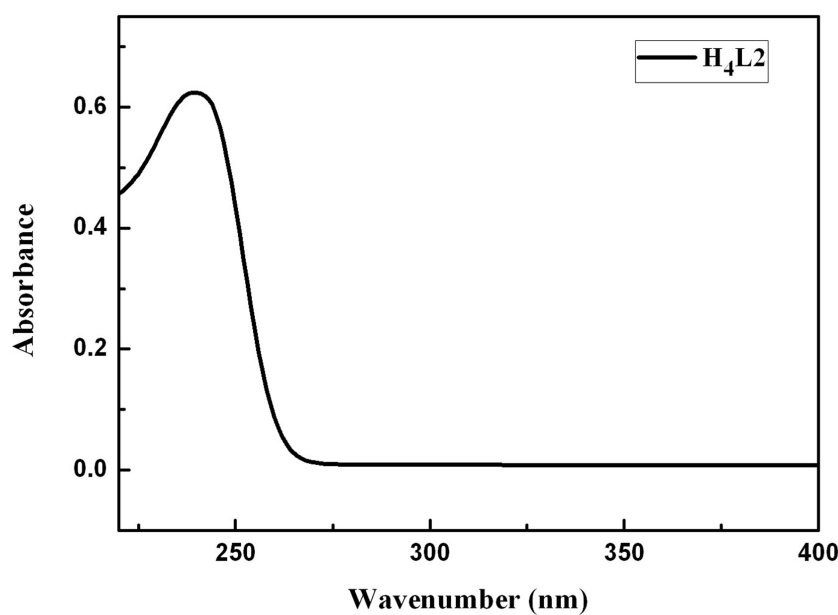


Figure S15 UV-visible spectrum for $\text{H}_4\text{L}1$ in aqueous solution.

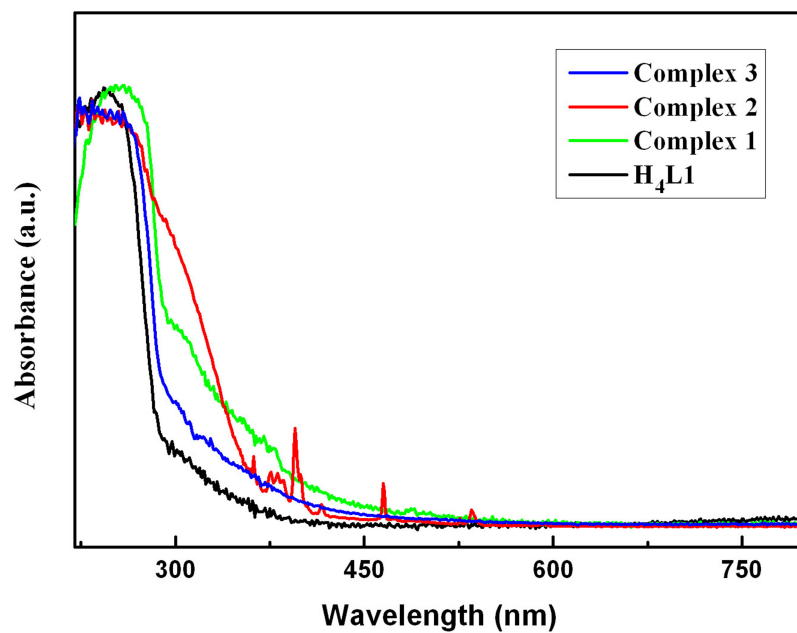


Figure S16 UV-visible spectrum for complex **1**(green), **2** (red), **3** (blue) and $\text{H}_4\text{L}1$ (black) in solid state.

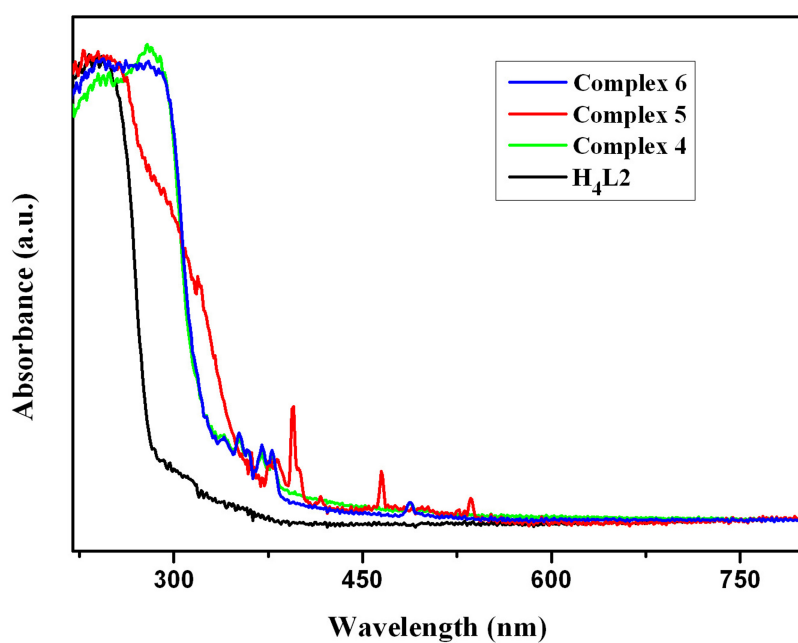


Figure S17 UV-visible spectrum for complex **4**(green), **5** (red), **6**(blue) and H₄L2 (black) in solid state.

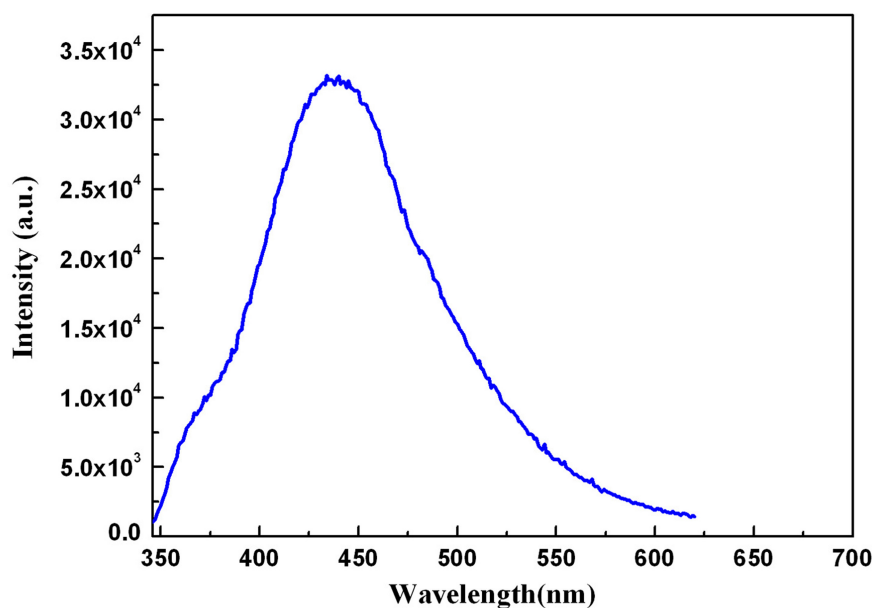


Figure S18 Solid-state emission spectrum of complex **3** excited at 352 nm.

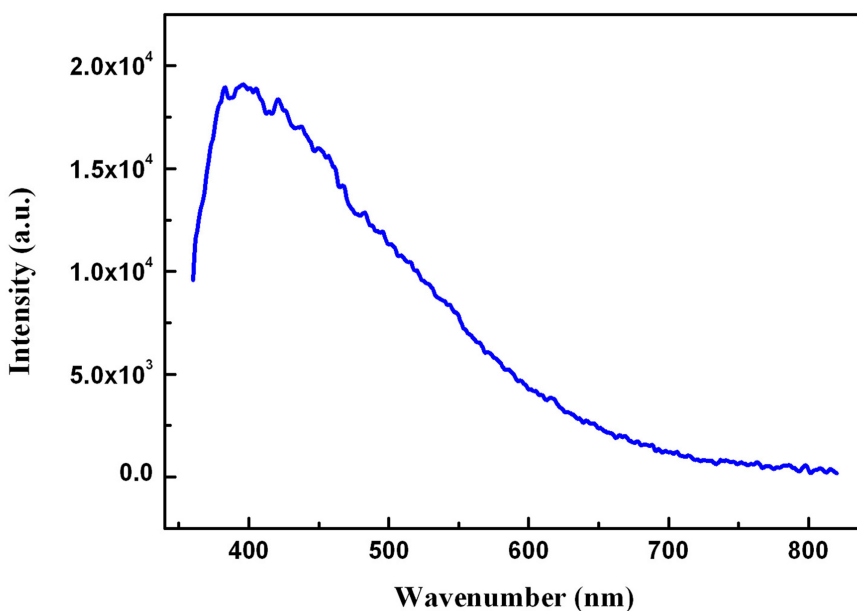


Figure S18 Solid-state emission spectrum of complex **6** excited at 342 nm.

Table S1. Selected Bond lengths (Å) and Angles (deg) for Complex 1

Tb(1)-Tb(1)c	3.8778(7)	O(7)a-Tb(1)-O(4)	127.1(2)	O(7)a-Tb(1)-O(3)	74.9(2)
Tb(1)-O(7)a	2.290(7)	O(2)a-Tb(1)-O(4)	155.8(2)	O(2)a-Tb(1)-O(3)	141.0(2)
Tb(1)-O(2)a	2.328(5)	O(8)b-Tb(1)-O(4)	87.9(2)	O(8)b-Tb(1)-O(3)	139.7(2)
Tb(1)-O(8)b	2.379(6)	O(1)b-Tb(1)-O(4)	69.8(2)	O(1)b-Tb(1)-O(3)	75.5(2)
Tb(1)-O(1)b	2.453(6)	O(7)a-Tb(1)-O(6)	82.9(2)	O(4)-Tb(1)-O(3)	53.4(2)
Tb(1)-O(4)	2.451(6)	O(2)a-Tb(1)-O(6)	81.5(2)	O(6)-Tb(1)-O(3)	71.4(3)
Tb(1)-O(6)	2.464(7)	O(8)b-Tb(1)-O(6)	125.3(2)	O(5)-Tb(1)-O(3)	101.8(2)
Tb(1)-O(5)	2.465(6)	O(1)b-Tb(1)-O(6)	146.9(2)	O(7)a-Tb(1)-O(2)b	71.2(2)
Tb(1)-O(3)	2.467(7)	O(4)-Tb(1)-O(6)	89.8(2)	O(2)a-Tb(1)-O(2)b	76.1(2)
Tb(1)-O(2)b	2.593(6)	O(7)a-Tb(1)-O(5)	133.2(2)	O(8)b-Tb(1)-O(2)b	70.4(2)
O(7)a-Tb(1)-O(2)a	74.4(2)	O(2)a-Tb(1)-O(5)	82.6(2)	O(1)b-Tb(1)-O(2)b	50.97(18)
O(7)a-Tb(1)-O(8)b	137.4(2)	O(8)b-Tb(1)-O(5)	73.7(2)	O(4)-Tb(1)-O(2)b	118.69(19)
O(2)a-Tb(1)-O(8)b	79.1(2)	O(1)b-Tb(1)-O(5)	136.3(2)	O(6)-Tb(1)-O(2)b	149.4(2)
O(7)a-Tb(1)-O(1)b	89.0(2)	O(4)-Tb(1)-O(5)	74.1(2)	O(5)-Tb(1)-O(2)b	141.0(2)
O(2)a-Tb(1)-O(1)b	127.0(2)	O(6)-Tb(1)-O(5)	53.4(2)	O(3)-Tb(1)-O(2)b	115.3(2)
O(8)b-Tb(1)-O(1)b	81.1(2)				

Symmetry codes: a: -x-1/2, y-1/2, -z-1/2; b: x, -y, z+1/2; c: -x-1/2, y-1/2, -z.

Table S2. Selected Bond lengths (Å) and Angles (deg) for Complex 4

Tb(1)-Tb(1)b	4.050(2)	O(5)a-Tb(1)-O(3)b	78.56(12)	O(5)a-Tb(1)-O(3)	137.14(12)
Tb(1)-O(7)a	2.253(3)	O(9W)-Tb(1)-O(3)b	89.14(19)	O(9W)-Tb(1)-O(3)	79.8(2)

Tb(1)-O(5)a	2.310(3)	O(7)a-Tb(1)-O(1)c	83.89(15)	O(3)b-Tb(1)-O(3)	65.85(12)
Tb(1)-O(9W)	2.331(5)	O(5)a-Tb(1)-O(1)c	134.43(13)	O(1)c-Tb(1)-O(3)	77.48(14)
Tb(1)-O(3)b	2.357(3)	O(9W)-Tb(1)-O(1)c	148.68(15)	O(2)c-Tb(1)-O(3)	113.60(14)
Tb(1)-O(1)c	2.425(4)	O(3)b-Tb(1)-O(1)c	100.74(15)	O(7)a-Tb(1)-O(4)	79.57(12)
Tb(1)-O(2)c	2.449(4)	O(7)a-Tb(1)-O(2)c	88.70(15)	O(5)a-Tb(1)-O(4)	145.40(13)
Tb(1)-O(3)	2.467(3)	O(5)a-Tb(1)-O(2)c	82.02(13)	O(9W)-Tb(1)-O(4)	73.51(15)
Tb(1)-O(4)	2.502(3)	O(9W)-Tb(1)-O(2)c	157.83(15)	O(3)b-Tb(1)-O(4)	117.44(10)
O(7)a-Tb(1)-O(5)a	86.48(13)	O(3)b-Tb(1)-O(2)c	81.24(14)	O(1)c-Tb(1)-O(4)	75.58(12)
O(7)a-Tb(1)-O(9W)	95.3(2)	O(1)c-Tb(1)-O(2)c	53.39(12)	O(2)c-Tb(1)-O(4)	128.63(12)
O(5)a-Tb(1)-O(9W)	76.49(17)	O(7)a-Tb(1)-O(3)	131.13(12)	O(3)-Tb(1)-O(4)	52.21(10)
O(7)a-Tb(1)-O(3)b	162.96(12)				

Symmetry codes: a: x, y, z-1, b: -x+1, -y, -z, c: x, -y-1/2, z-1/2

Table S3. Selected Bond lengths (Å) and Angles (deg) for Complex 5

Eu(1)-Eu(1)b	4.094(2)	O(5)a-Eu(1)-O(3)b	78.4(2)	O(5)a-Eu(1)-O(3)	137.4(2)
Eu(1)-O(7)a	2.279(6)	O(9W)-Eu(1)-O(3)b	88.0(3)	O(9W)-Eu(1)-O(3)	78.7(3)
Eu(1)-O(5)a	2.330(5)	O(7)a-Eu(1)-O(1)c	83.7(3)	O(3)b-Eu(1)-O(3)	66.2(2)
Eu(1)-O(9W)	2.340(8)	O(5)a-Eu(1)-O(1)c	134.8(2)	O(1)c-Eu(1)-O(3)	77.3(2)
Eu(1)-O(3)b	2.387(6)	O(9W)-Eu(1)-O(1)c	147.8(3)	O(2)c-Eu(1)-O(3)	112.8(2)
Eu(1)-O(1)c	2.467(6)	O(3)b-Eu(1)-O(1)c	101.4(2)	O(7)a-Eu(1)-O(4)	79.7(2)
Eu(1)-O(2)c	2.490(6)	O(7)a-Eu(1)-O(2)c	89.2(2)	O(5)a-Eu(1)-O(4)	145.5(2)
Eu(1)-O(3)	2.499(6)	O(5)a-Eu(1)-O(2)c	83.1(2)	O(9W)-Eu(1)-O(4)	73.2(2)
Eu(1)-O(4)	2.528(5)	O(9W)-Eu(1)-O(2)c	159.1(2)	O(3)b-Eu(1)-O(4)	117.11(18)
O(7)a-Eu(1)-O(5)a	86.5(2)	O(3)b-Eu(1)-O(2)c	81.5(2)	O(1)c-Eu(1)-O(4)	75.1(2)
O(7)a-Eu(1)-O(9W)	96.2(3)	O(1)c-Eu(1)-O(2)c	52.78(19)	O(2)c-Eu(1)-O(4)	127.66(19)
O(5)a-Eu(1)-O(9W)	77.1(3)	O(7)a-Eu(1)-O(3)	130.63(19)	O(3)-Eu(1)-O(4)	51.56(17)
O(7)a-Eu(1)-O(3)b	163.1(2)				

Symmetry codes: a: x, y, z-1, b: -x+1, -y, -z, c: x, -y-1/2, z-1/2

Table S4. Selected Bond lengths (Å) and Angles (deg) for Complex 6

Gd(1)-Gd(1)b	4.0724(14)	O(5)a-Gd(1)-O(3)b	79.1(3)	O(5)a-Gd(1)-O(2)c	82.5(3)
Gd(1)-O(7)a	2.265(7)	O(9W)-Gd(1)-O(3)b	88.7(4)	O(9W)-Gd(1)-O(2)c	158.2(3)
Gd(1)-O(5)a	2.317(7)	O(7)a-Gd(1)-O(1)c	83.3(3)	O(3)b-Gd(1)-O(2)c	82.0(3)
Gd(1)-O(9W)	2.343(10)	O(5)a-Gd(1)-O(1)c	134.6(3)	O(1)c-Gd(1)-O(2)c	53.3(3)
Gd(1)-O(3)b	2.375(7)	O(9W)-Gd(1)-O(1)c	148.5(3)	O(3)-Gd(1)-O(2)c	113.1(3)
Gd(1)-O(1)c	2.451(9)	O(3)b-Gd(1)-O(1)c	101.5(3)	O(7)a-Gd(1)-O(4)	79.5(3)
Gd(1)-O(3)	2.464(8)	O(7)a-Gd(1)-O(3)	130.8(3)	O(5)a-Gd(1)-O(4)	145.2(3)
Gd(1)-O(2)c	2.468(8)	O(5)a-Gd(1)-O(3)	137.6(3)	O(9W)-Gd(1)-O(4)	73.4(3)
Gd(1)-O(4)	2.520(7)	O(9W)-Gd(1)-O(3)	80.1(4)	O(3)b-Gd(1)-O(4)	116.7(2)
O(7)a-Gd(1)-O(5)a	86.5(3)	O(3)b-Gd(1)-O(3)	65.4(3)	O(1)c-Gd(1)-O(4)	75.4(3)
O(7)a-Gd(1)-O(9W)	95.3(4)	O(1)c-Gd(1)-O(3)	77.4(3)	O(3)-Gd(1)-O(4)	52.0(2)
O(5)a-Gd(1)-O(9W)	76.4(3)	O(7)a-Gd(1)-O(2)c	88.8(3)	O(2)c-Gd(1)-O(4)	128.4(3)

O(7)a-Gd(1)-O(3)b 163.7(3)

Symmetry codes: a: x, y, z-1, b: -x+1,-y, -z, c: x,-y-1/2, z-1/2

References

1. P. de Hoog, P. Gamez, W. L. Driessens and J. Reedijk, *Tetrahedron Lett.* **2002**, *43*, 6783.